A Retinoic Acid-dependent Stroma-Leukemia Crosstalk Promotes Chronic Lymphocytic Leukemia

Progression


Farinello et al.


A Retinoic Acid-dependent Stroma-Leukemia Crosstalk Promotes Chronic Lymphocytic Leukemia

Progression

# Supplementary table 1: primary antibodies for immunofluorescence and FACS

| Antibody | Species | Conjugation | Company | Dilution | Clone / Cat. no. |
|---|---|---|---|---|---|
| CD19 | Rat | PE | BD pharmingen | 1:50 for FACS | Clone 1D3 / Cat. no. 553786 |
| CD5 | Rat | APC | BD pharmingen | 1:50 for FACS | Clone 53-7.3 / Cat. no. 550035 |
| CD35 | Rat | Biotinylated | BD pharmingen | 1:100 | Clone 8C12 / Cat. no. 553816 |
| Collagen IV | Rabbit | - | Abcam | 1:500 | Cat. no. Ab19808 |
| CXCL13 (for mouse) | Goat | - | R&D systems | 1:100 | Cat. no. AF470 |
| Nidogen 2 | Rabbit | - | Abcam | 1:500 | Cat. no. Ab14513 |
| Laminin | Rabbit | - | Sigma Aldrich | 1:300 | Cat. no. L9393 |
| MadCAM-1 | Rat | Biotinylated | BD pharmingen | 1:50 | Clone MECA-367 / Cat. no. 553808 |
| MOMA-1 | Rat | Biotinylated | Abcam | 1:500 | Cat. no. Ab51814 |
| CD21/35 | Rabbit | PE | eBioscience | 1:100 | Clone 4E3/ Cat. no. 12-0212 |
| GFP | Rabbit | - | Abcam | 1:500 | Cat. no. ab13970 |
| CXCL13 (for human) | Goat | - | R&D systems | 1:30 | Cat. no. AF801 |
| IgD (for human) | Goat | Biotinylated | SouthernBiotech | 1:100 | Cat. no. 2030-08 |
| MAdCAM (for human) | Mouse | - | Serotech | 1:100 | Clone 314G8 Cat. no. |

## Supplementary table 2: secondary reagents

| Antigen | Fluorochrome | Company | Dilution | Cat. no. |
|---|---|---|---|---|
| Anti-goat | Biotinylated | Vector | 1:500 | BA-9500 |
| Anti-rabbit | Alexa Fluor 546 | Invitrogen | 1:500 | A-11035 |
| Anti-mouse | Alexa Fluor 568 | Invitrogen | 1:500 | A-11031 |
| Anti-rabbit | Alexa Fluor 488 | Invitrogen | 1:500 | A-21441 |
| Anti-rabbit | Alexa Fluor 647 | Invitrogen | 1:500 | A-31573 |
| Anti-rat | Alexa Fluor 488 | Invitrogen | 1:500 | A-21208 |
| Streptavidin | HRP | Perkin Elmer | 1:500 | NEL750 |
| Streptavidin | Alexa Fluor 546 | Invitrogen | 1:500 | S11225 |
| Streptavidin | Alexa Fluor 488 | Invitrogen | 1:500 | S11223 |
| Streptavidin | Alexa Fluor 647 | Invitrogen | 1:500 | S21374 |

**Supplementary table 3:** Sequence of Specific Primers and Probes Used for qPCR Analysis (Probe number corresponds to Universal Probe Library – Roche)

| Gene | Forward Sequence | Reverse Sequence | Probe N° | Species |
|------|------------------|------------------|----------|---------|
| Aldh1a1 | GCTGAACAAGCTGGCTGAC | CCATTGAGTGCCTCCATTGTA | #84 | M. Musculus |
| Atraid | TGAGGATACATCGAAGCTAATGC | AGGGAACAGTTCTGAAGATCTAGC | #27 | M. Musculus |
| Col1a1 | ACCTAAGGGTACCGCTGGA | GAGCTCCAGCTTCTCCATCTT | #18 | M. Musculus |
| Col3a1 | ACCTCCTGGTGCTCTTGGT | CACGCTCTCCAGGTCGTC | #58 | M. Musculus |
| Col4a6 | CAGCCTCTGGATCGGATACT | ACTAGGGACTGGCCTCCAC | #3 | M. Musculus |
| Cyp1b1 | GGAAACCACGCTTCATCG | AGGACGGAGAAGAGTAGCAGAA | #84 | M. Musculus |
| Cxcl12 | CCAAACTGTGCCCTTCAGAT | CTTTAGCTTCGGGTCAATGC | #41 | M. Musculus |
| Cxcl13 | TGAGGCTCAGCACAGCAA | ATGGGCTTCCAGAATACCG | #84 | M. Musculus |
| Itga1 | GACTGACGTGACCATTGGAG | TGGTCACTTTAACTACAGCCACA | #17 | M. Musculus |
| Lama5 | GAGTCTGTGCGAGCTGTGG | TCGCCAGACGGTACCAAG | #80 | M. Musculus |
| Loxl2 | AGCTTTTCTTCTGGGCAACC | CTCCATCCTTGTCCTGTGCT | #18 | M. Musculus |
| Nidogen-2 | TGAGGCAGCTATCTGCTACAAT | CTTCCGGAACCGTGTCAG | #64 | M. Musculus |
| Prelp | CAGAAGAGTGCCCCAGAGTC | ATGCCCTCATGATCCAGGT | #91 | M. Musculus |
| Rdh10 | CTCCCTGGGACTGTTCAGC | TCGTGAAAACCCACAACTCC | #67 | M. Musculus |
| Rarbeta | CACCGGCATACTGCTCAA | CAAACGAAGCAGGGCTTG | #63 | M. Musculus |
| Rargamma (isoform2) | CGCCGGACTTGAGTCTTTT | GCTCTGTGTCTCCACCGATT | #104 | M. Musculus |
| qSma | TCACCATTGGAAACGAACG | ATAGGTGGTTTCGTGGATGC | #11 | M. Musculus |
| Vcam-1 | TGGTGAAATGGAATCTGAACC | CCCAGATGGTGGTTTCCTT | #34 | M. Musculus |
| Rpl13a | CCCTCCACCCTATGACAAGA | GTAGGCTTCAGCCGAACAAC | #63 | M. Musculus |
| | | | | |
| RXRalpha | AAGCGGATCCCACACTTCT | GAAGGAGGCGATGAGCAG | 18 | H. Sapiens |
| Gapdh | AGCCACATCGCTCAGACAC | GCCCAATACGACCAAATCC | 60 | H. Sapiens |

| Vgll4 | Nid2 | C3, |
| Bst2 | Crim1 | Cd59a |
| Ifit3 | Agrn | Cd74 |
| Isg15 | Cyr61 | Crim1 |
| Aldh3b1 | Gas6 | F11r |
| Lgals3bp | Acta2 | Gadd45g |
| Vamp5 | Ogn | Hp |
| Psme1 | Prelp | Ier3 |
| Aldh1a1 | Serpina3n | Il6st |
| Usp18 | Serpinb6b | Lamb2 |
| Cyp1b1 | Plau | Rgs16 |
| Actg2 | Sema3f | Trex1 |
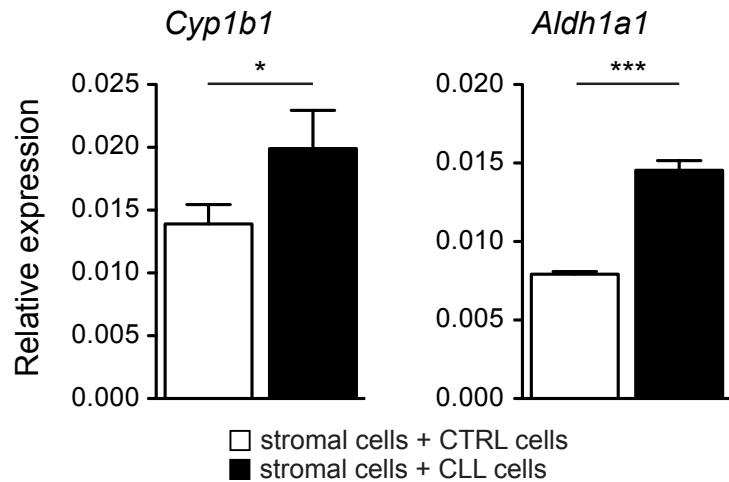
**Supplementary Figure 1. Leukemic cells induce the expression of genes involved in RA-synthesis and tissue remodeling.**
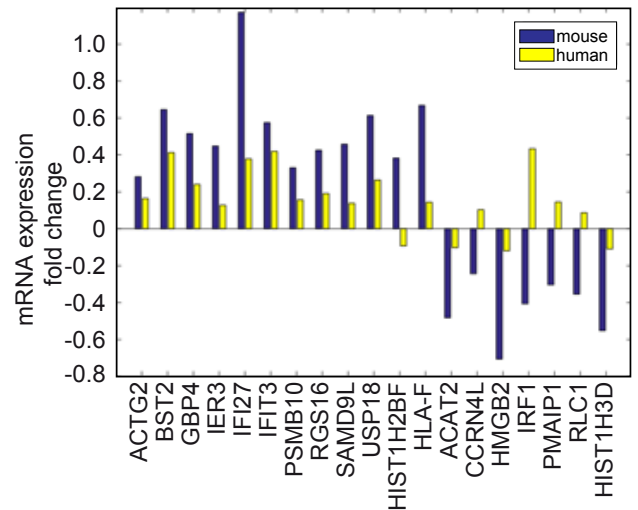List of selected gene-signatures deregulated in stromal cells (mSSC) after the co-culture with murine *Eμ-TCL1* CLL or CTRL (splenic B cells) cells. In red are highlighted genes involved in RA synthesis, and Cyp1b1 and Aldh1a1 were validated by qPCR analysis. Data are from one out of four independent experiments with similar results. The mean of triplicates and ± SD are shown; * p < 0.05, *** p < 0.001.
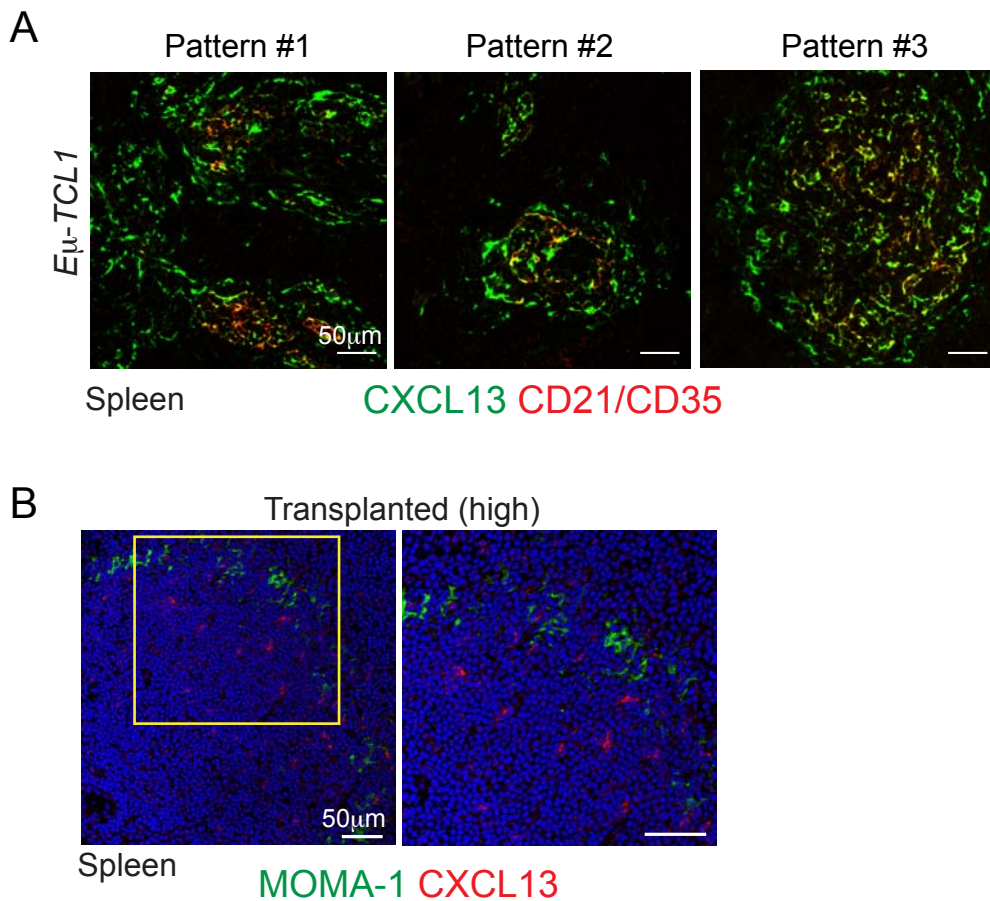
Farinello et al., Figure S1

**Supplementary Figure 2. Murine and human stroma-specific gene signature induced by human CLL.**
A) qPCR analysis of stroma-specific genes from a murine stromal cell line (mSSC) cultured with human primary CLL cells for 24 hrs. B) Fold change comparison of common genes deregulated in stromal cells by mouse (our microarray data) and human CLL cells (from Paggetti et al. dataset).
Annotations of stromal-gene signatures by human CLL cells revealed similarities between mouse and human.
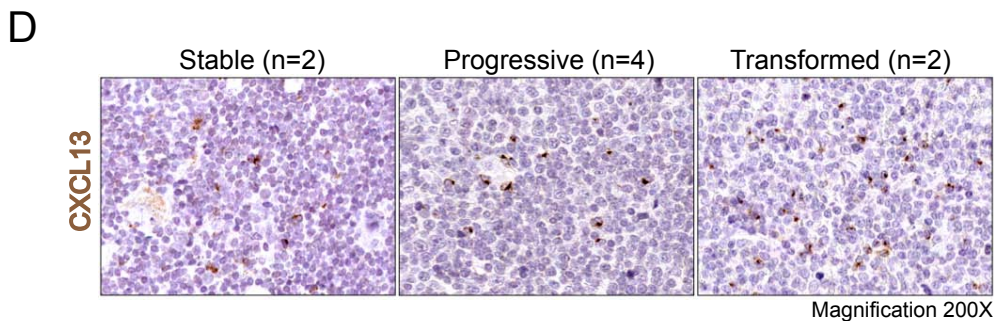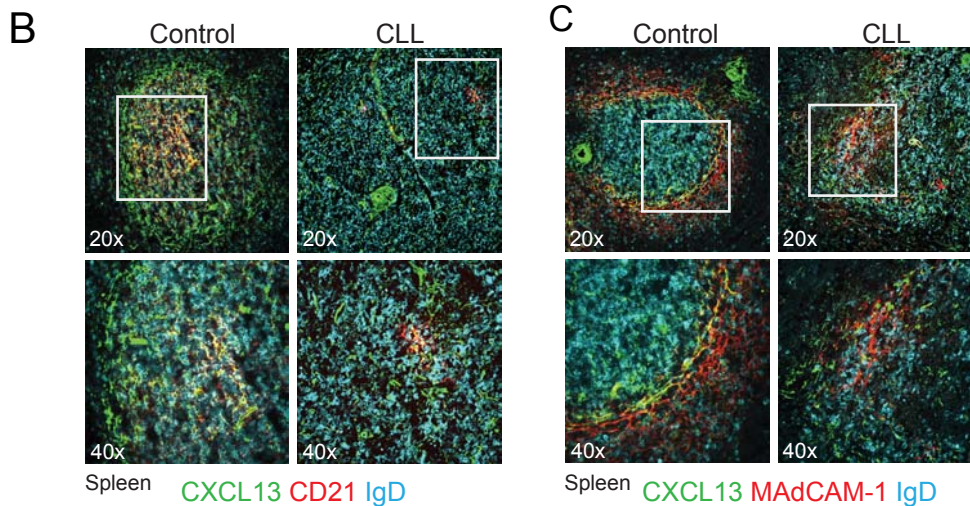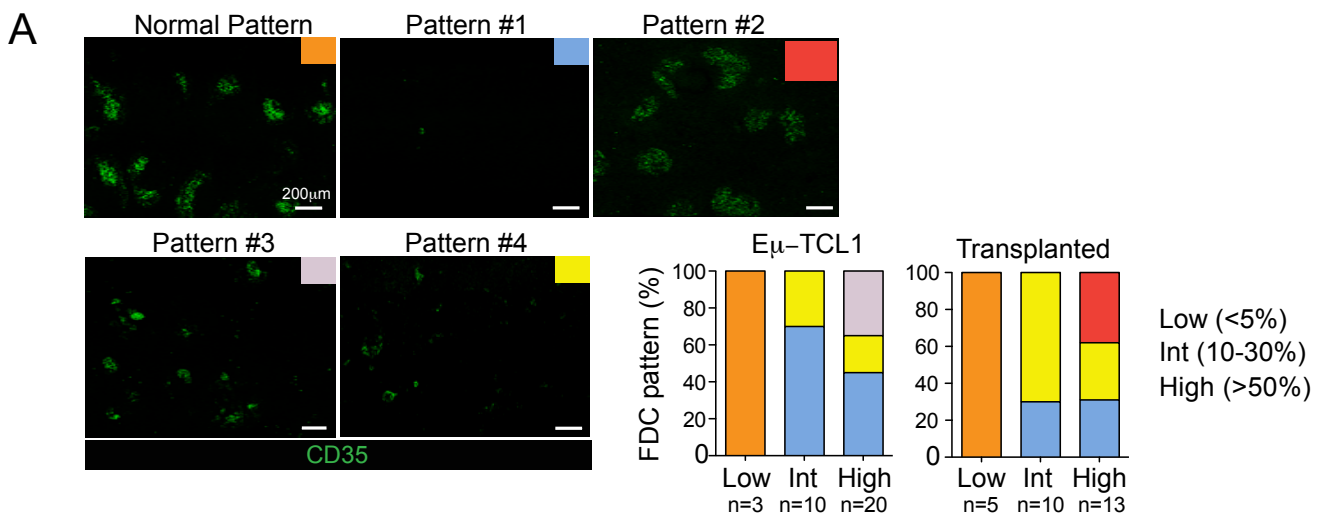
Farinello et al., Figure S2

**Supplementary Figure 3. A fraction of leukemic cells possess ALDH activity.**
*Eμ-TCL1* leukemia cells isolated from the spleen of five different leukemia-bearing mice and two control mice were assessed for Aldefluor activity in the absence or presence of the ALDH control inhibitor (DEAB). One representative analysis is shown (highlighted row).

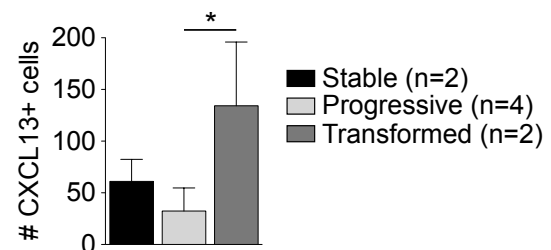| MOUSE | STRAIN | ALDEFLUOR+/CD19+ | ALDEFLUOR+/CD19+ with DEAB | ALDEFLUOR+/CD19+CD5+ | ALDEFLUOR+/CD19+CD5+ with DEAB |
|---|---|---|---|---|---|
| WT1 | C57BL6 | 0.999 | 0.313 | 3.17 | 1.2 |
| WT2 | C57BL6 | 0.135 | 0.0215 | 0.532 | 0.233 |
| TCL1 #1 | Eμ-TCL1 | 5.45 | 0.011 | 20.9 | 0.094 |
| TCL1 #2 | Eμ-TCL1 | 14 | 1.21 | 30.3 | 0.52 |
| TCL1 #3 | Eμ-TCL1 | 4.54 | 0.0807 | 10.2 | 0.0861 |
| TCL1 #4 | Eμ-TCL1 | 8.93 | 0.0219 | 19.2 | 0.104 |
| TCL1 #5 | Eμ-TCL1 | 15.6 | 1.2 | 17.5 | 0.3 |

Farinello et al., Figure S3

**Supplementary Figure 4. Distribution of CXCL13 in spleen follicular stromal cells but not in macrophages.**
A) Confocal images of the spleen stained for CXCL13 (green) and CD21/CD35 (red) to visualize follicular stromal cells. B) Confocal image of the spleen from transplanted mice with high infiltration of leukemic cells stained for MOMA-1 (green) to visualize marginal metallophilic macrophages, and CXCL13 (red) to visualized reticular stromal cells. Data are representative of one out of five mice analyzed. Scale bars represent 50μm.

A) Representative confocal mosaic images of spleen sections. Tissues were isolated from transgenic and transplanted mice with low (<5%), intermediate (10-30%) and high (>50%) leukemia infiltration and stained for CD35 (green) to visualized FDCs. Graphs indicate the frequency of the different FDC patterns. Scale bars represent 200μm.
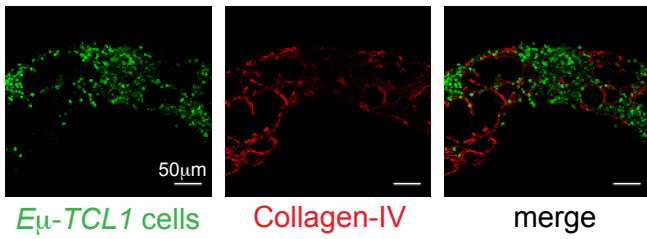
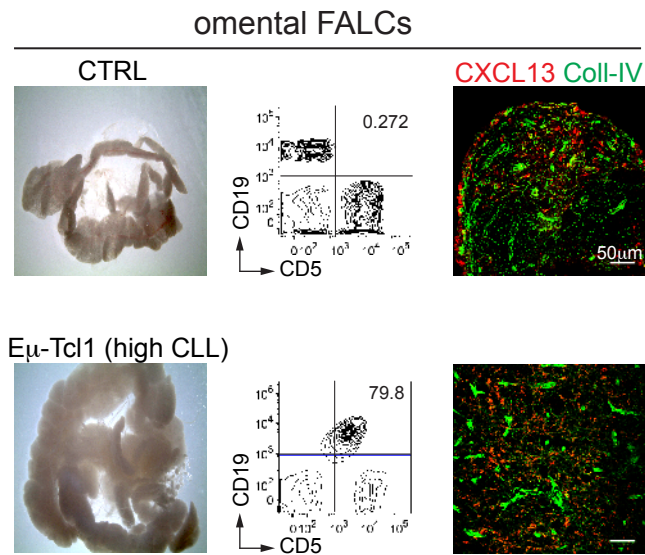**Supplementary Figure 5. Leukemia-stroma interactions cause disorganization of the follicular architecture.** A) Representative confocal mosaic images of spleen sections. Tissues were isolated from transgenic and transplanted mice with low (<5%), intermediate (10-30%) and high (>50%) leukemia infiltration and stained for CD35 (green) to visualized FDCs. Graphs indicate the frequency of the different FDC patterns. Scale bars represent 200μm. B-C) Representative confocal images of human CLL spleens and controls stained for CXCL13 (green) and CD21 (red) and MAdCAM-1(red) to visualize FDC and MRC stromal cells respectively, and IgD (light blue) to visualize B cells. Original magnifications: 20X and 40x (insets). D) Bright field images of human CLL lymph node sections stained for CXCL13 (brown). Graph represents the average number of CXCL13+ cells from five high power fields (HPF) for each sample. Original magnification: 200x.
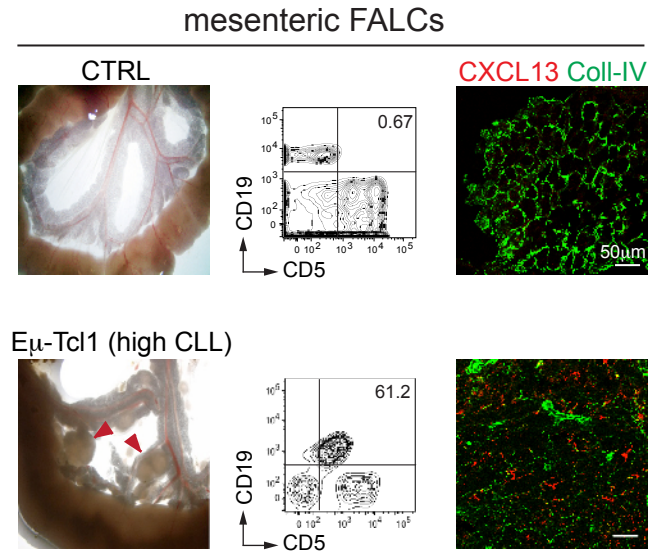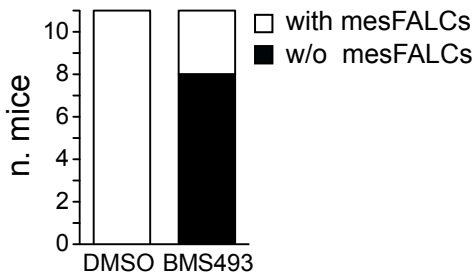
Farinello et al., Figure S5

**A**

*Eμ-TCL1* cells     Collagen-IV     merge

**B**    omental FALCs

CTRL       CXCL13 Coll-IV

0.272

Eμ-Tcl1 (high CLL)

79.8

**C**    mesenteric FALCs

CTRL       CXCL13 Coll-IV

0.67

Eμ-Tcl1 (high CLL)

61.2

**D**

☐ with mesFALCs
■ w/o mesFALCs

**Supplementary Figure 6. Fat-associated lymphoid clusters support leukemia expansion and are inhibited by retinoid-antagonist therapy**.
A) Representative confocal images of omental FALCs from wild type mice injected with CMFDA-labeled *Eμ-TCL1* CLL cells (green) and stained for collagen-IV (red). Scale bars represent 50μm. B-C) Representative bright-field images, flow cytometry plots showing CD5 and CD19 staining, and representative confocal images stained for CXCL13 (red) and Collagen-IV (green) from control or leukemic *Eμ-TCL1* mice with high percentage of leukemia in the blood. Scale bars represent 50μm. Data are representative of one out of five mice analyzed for each group. D) Number of mice treated with DMSO or BSM493 showing induction of mesenteric FALCs.

Farinello et al., Figure S6